

## Experimental Electron-Transfer Cross Sections for Collisions of Oxygen Ions in Argon, Nitrogen, and Helium at Energies of 7–40 MeV

J. R. Macdonald\*

*Niels Bohr Institute, Copenhagen, Denmark*

and

F. W. Martin†

*Institute of Physics, University of Aarhus, Aarhus, Denmark*

(Received 3 May 1971)

In the energy range 7–40 MeV, electron-capture and electron-loss cross sections have been determined for incident oxygen ions of charges +2 to +8 passing through argon, nitrogen, and helium. Thin-target conditions have been used in all cases. The analysis technique used to extract the cross sections allows relative cross sections to be obtained without consideration of the measurement of the gas target thickness. Multiple-transfer cross sections can thereby be determined reliably in the presence of cross sections three orders of magnitude greater. Double, triple, and quadruple transfers were observed. The electron-loss cross sections appear to pass through maxima when the velocity of the ion is in the vicinity of the velocity of the electron to be lost. Single-electron-capture cross sections have magnitudes as large as  $10^{-17}$  cm<sup>2</sup> at 40 MeV in argon, and depend on velocity approximately as  $V^{-n}$ , where  $n$  lies between 3 and 6 for the heavy gases. The importance of capture from inner shells of the heavy gases is inferred by comparison with helium, in which  $n$  is 8 or 9 and the cross sections are relatively small. The possibility of capture into the  $K$  shell of the oxygen ion is suggested by the systematic differences observed in capture by +7 and +8 oxygen ions from capture by lower-charged ions.

### I. INTRODUCTION

When a beam of swift atomic projectiles passes through matter, electrons are captured or lost in successive collisions, causing a fluctuation in the charge of a given ion and a statistical distribution of charge states in the ion beam. Most experimenters have investigated only the charge-state distributions, since the mean-square charge resulting from charge-changing collisions is of importance in determining the stopping of very fast heavy ions. If more than a phenomenological understanding of the effects observed in these distributions is to be obtained, however, the cross sections for individual charge-changing collisions must be investigated. In addition to their connection with stopping processes, these atomic-collision cross sections have a high degree of intrinsic interest and are also useful in astrophysics, cosmic-ray studies, and heavy-ion accelerator design.

For collisions in rarefied gases, the cross sections  $\sigma_{ij}$  for a projectile with initial and final charge states  $i$  and  $j$  are generally well defined at a specific energy since the energy is not significantly decreased in a single collision. Early work on collisions involving hydrogen and helium projectiles has been reviewed by Allison<sup>1</sup>; and more recently, reviews by Northcliffe<sup>2</sup> and Nikolaev<sup>3</sup> have included electron capture and loss by heavier atoms. In recent measurements,<sup>4–8</sup> charge-transfer cross sec-

tions have been determined in the energy region above 1 MeV/amu, and the present experiment<sup>9</sup> provides data in the region 0.5–2.5 MeV/amu. The cross sections were obtained for oxygen ions of charge +2 to +8 by measuring the growth of various charge states in a thin target of argon, nitrogen, or helium when a beam of single known charge was incident.

### II. APPARATUS

The experimental apparatus constructed for this work is shown schematically in Fig. 1. Oxygen ions of an appropriate charge were accelerated to the required energy in the Tandem Van de Graaff accelerator of the Niels Bohr Institute. The energy was determined by a calibrated energy analyzing magnet, with its magnetic field determined by proton nuclear magnetic resonance. Estimated systematic and random errors in energy were 0.5%. A series of energies could be rapidly obtained by keeping the field in the analyzing magnet constant while adjusting the accelerating voltage so that ions were transmitted in charge states from +6 to +2.

After passing through the energy analyzing magnet, the beam traversed a thin carbon foil, approximately 30  $\mu\text{g}/\text{cm}^2$  in weight, which produced a distribution of charge states, all of the same energy. At any energy, a single one of these charge states could be deflected into the collision chamber using the beam switching magnet. The path length

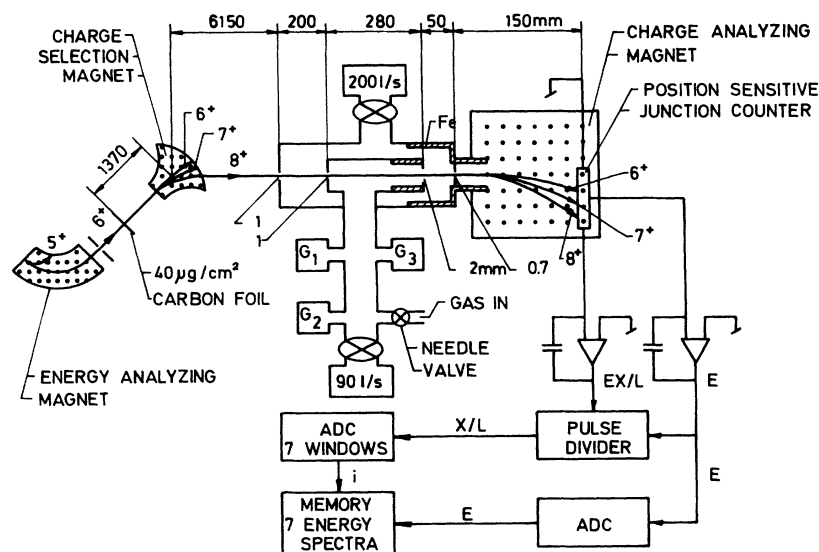


FIG. 1. Schematic diagram of experimental apparatus for the measurement of charge-exchange cross sections at MeV energies. The differentially pumped target chamber was 28 cm long.

from the foil to the collision chamber was 7.8 m and the trajectory in the magnet was a  $30^\circ$  arc of 1.1-m radius, beginning 1.0 m after the foil. With no gas in the collision chamber, the pressure of residual gas in this region was approximately  $3 \times 10^{-6}$  Torr, corresponding to  $10^{14}$  atoms/cm<sup>2</sup> and a typical measured purity of 97 to 99% in the incident charge state.

The 28-cm-long differentially pumped collision chamber was connected to a gas-handling manifold that could be pumped directly by an oil diffusion pump with a speed of about 90 liter sec<sup>-1</sup>. The target gases, specified to be less than 0.01% impure by the manufacturer, were admitted through a commercial "needle" valve (consisting of a carefully machined steel rod protruding a variable distance into a cylindrical hole). With no gas flow, the residual pressure was less than  $10^{-5}$  Torr, while the typical operating pressures were in the  $10^{-3}$ -Torr region. A contamination of the target gases of less than 1% from out gassing and leaks is therefore estimated. To obtain high pressures it was necessary to partially or completely close a valve over the diffusion pump; however, the flow through the needle valve was still maintained large relative to the flow of possible contaminant in this case.

Pressures of argon in the collision chamber were initially measured with a specially constructed high-pressure ion gauge,<sup>10</sup> which was calibrated against a McLeod gauge trapped with liquid nitrogen. Pressures of nitrogen, helium and in some cases argon were measured directly with the McLeod gauge. A correction for the pumping effect of the liquid-nitrogen trap was made using the expressions of Meinke and Reich.<sup>11</sup> The maximum correction was 20% for argon at low pressure; typical corrections were much smaller. For pressures at which most

cross sections were determined, it is estimated that the absolute uncertainty in gas target thickness is about 10%, although there is a smaller relative uncertainty between different target thicknesses.

The ions emerging from the collision chamber in several charge states were deflected in an analyzing magnet, and all charge states were detected simultaneously in a position-sensitive silicon junction detector 30 mm in length.<sup>12</sup> With the detector located between the poles of the magnet, approximately 10 cm from the edge, the deflection was nearly proportional to the charge of the ions, and a separation of 3 mm was normally used between adjacent charge states. Dimensions of the collimating system are shown in Fig. 1. Each collimator except the one fixed to the magnet was separately adjustable, and all were aligned to about 0.1 mm using a telescope behind the steering magnet. At high energies, where multiple scattering was negligible, the resulting distribution of ions on the detector was several 0.5-mm-diam uniform circles. At low energies the circles became larger and nonuniform. Systematic error introduced by the varying deflection of the different charge states between the last two collimators was eliminated by shielding the entire path from the fringing field of the analyzing magnet.

From the position-sensitive detector, two pulses were obtained, one proportional to the particle energy and the other to the product of energy and position. True position pulses were obtained by dividing the latter by the former in an analog divider circuit. The charge distribution was obtained by analyzing the position and energy pulses in a 4096-channel pulse-height analyzer operated in an eight-channel sorting mode. In this mode, events with position pulses falling within one of eight

"windows" caused the energy pulse to be added to one of eight 512-channel spectra. Only the sum of counts in each spectrum, corresponding to the total number of counts in each charge state, was printed out.

Usually  $10^5$  ions were counted at a rate of  $10^3$  per sec for each incident charge state at each gas pressure and particle energy. A typical emergent distribution consisted of  $9 \times 10^4$  counts in the initial state,  $10^4$  counts distributed among the adjoining four states, and on the order of 100 background counts in each of the remaining states, presumably caused by slit-edge scattering on the 0.5-mm aperture. The background set a limit of 0.001 for the smallest charge state fraction which could be detected. For a charge state at this limit the probable error from counting statistics alone was 10% or 0.0001, while for a charge state fraction equal to 0.1 it was 1% or 0.001.

The number of ions in each emergent charge state was measured for several incident charge states (typically +4 to +8) at a given setting of gas pressure. This procedure was repeated at enough additional gas pressures to ensure that four to five distributions were obtained in which the attenuation of each incident charge state was less than 20%. From these sets of charge fractions determined as a function of target thickness, the various electron-capture and electron-loss cross sections were extracted using the following data analysis.

### III. DATA ANALYSIS

#### A. Introduction

In general, the charge of a beam of ions passing through matter satisfies the differential equations

$$\frac{d\phi_i}{dx} = \sum_{j \neq i} (\sigma_{ji} \phi_j - \sigma_{ij} \phi_i), \quad (1)$$

where  $\phi_i$  is the fraction of projectiles with charge  $i$ ,  $x$  is the target thickness in atoms/cm<sup>2</sup>, and  $\sigma_{ij}$  is the cross section for a change in the ion charge from  $i$  to  $j$  in a collision with an atom.<sup>3</sup>

It is well known that the state of excitation of the ion has an effect on the magnitude of  $\sigma_{ij}$ , and effects of this type have been found for 12-MeV iodine ions<sup>13</sup> and 100-MeV carbon ions.<sup>8</sup> In the present experiment, a long flight path has been used in front of the target chamber in an attempt to minimize the excitation of the incident ions. For example, the time of flight of 40-MeV oxygen ions from the carbon foil to the collision chamber is  $3 \times 10^{-7}$  sec, and this is larger than the lifetime of  $2 \times 10^{-9}$  sec for the  $2^3P_1$  state of the +6 oxygen ion<sup>14</sup> as well as other measured lifetimes of oxygen ions.<sup>15</sup> In addition, many long-lived states in the incident beam can be expected to decay while passing through the charge selection magnet where the motional electric field appearing to the ions will

perturb and mix the states.

However, some excitations of the incident ion must result from collisions without charge exchange within the collision chamber. If the cross section for excitation is comparable to the sum of the charge-transfer cross sections, then charge exchange from the excited states will depend on the square of the target thickness; a first collision would produce the excited ion and a second collision would be necessary for charge transfer from the excited state. Such dependence was not found in the pressure range used in these experiments. However, if the excitation and deexcitation cross sections are one or more orders of magnitude larger than the transfer cross sections, then the beam would come to equilibrium with regard to excitation but not charge exchange. A linear dependence of charge transfer on target thickness would then occur with a cross section characteristic of the excited ions. In principle this possibility can be investigated by experiments at very small target thicknesses. No such study was attempted in the present work, and the cross sections must therefore be characterized by a typical gas pressure in the  $10^{-2}$ – $10^{-4}$  Torr range.

#### B. Method of Analysis

An approximate solution to Eq. (1) appropriate to thin-target experiments may be obtained for each incident charge state  $\alpha$  by assuming that the charge fraction  $\phi_\alpha$  is much larger than any of the  $\phi_i$  for  $i \neq \alpha$ . This assumption is approximately obeyed in this experiment, where  $\phi_\alpha(x) > 0.8$  and  $\phi_\alpha(0) > 0.97$ . In this case the terms containing  $\phi_j$  in Eq. (1) may be set equal to zero and the solutions may be written

$$\phi_\alpha(x) = \phi_\alpha(0) e^{-k_\alpha x}, \quad (2a)$$

$$\phi_i(x) = (\sigma_{\alpha i}/k_\alpha) [\phi_\alpha(0) - \phi_\alpha(x)] + \phi_i(0), \quad (2b)$$

where

$$k_\alpha = \sum_{j \neq \alpha} \sigma_{\alpha j}.$$

In the limiting case that  $\phi_\alpha(0) = 1$  and  $\phi_i(0) = 0$ , these solutions become

$$\phi_\alpha(x) = e^{-k_\alpha x}, \quad (3a)$$

$$\phi_i(x) = (\sigma_{\alpha i}/k_\alpha) (1 - \phi_\alpha), \quad i \neq \alpha. \quad (3b)$$

Clearly these approximate solutions will better correspond to the experimental situation in certain cases than in others. For example, if  $\sigma_{\alpha j} \geq 5\sigma_{j\alpha}$  for all  $j$ , then when  $\phi_\alpha \geq 0.8$ , as in these experiments,  $\sum_j \sigma_{j\alpha} \phi_j \leq 0.05 \sum_j \sigma_{\alpha j} \phi_\alpha$  and the terms from Eq. (1) neglected in Eq. (2) will lead to less than a 5% underestimate of the sum of the cross sections  $k_\alpha$ . However, if  $\sigma_{\alpha j} \sim \sigma_{j\alpha}$  for a particular  $j$ , then for  $\phi_\alpha \sim 0.8$  the terms  $\sum_j \sigma_{j\alpha} \phi_j \sim 0.25 \sum_j \sigma_{\alpha j} \phi_\alpha$  and

Eq. (2) will yield a 25% underestimate of  $k_\alpha$ . In other words, the transitions to the initial state from adjacent states will hinder the decay of the initial state, and  $\phi_\alpha(x)$  will have a different decay than that given by Eq. (2a). The largest error introduced in this manner will occur for the dominant charge states at each energy, that is, when  $\alpha$  is close to the most probable charge.

A second-order solution for  $\phi_\alpha(x)$  can be determined by using Eq. (3b) in Eq. (1) to decouple the differential equations, thereby approximating the feedback into the initial charge state as the target thickness increases. The second-order solution obtained for the incident charge state is

$$\phi_\alpha(x) = [\phi_\alpha(0)/(1 + a_\alpha)] \{ \exp[-k_\alpha(1 + a_\alpha)x] + a_\alpha \}, \quad (4a)$$

where

$$a_\alpha = (1/k_\alpha^2) \sum_{j \neq \alpha} \sigma_{\alpha j} \sigma_{j\alpha}. \quad (4b)$$

The analysis of all data and the extraction of the charge-exchange cross sections from the measured charge distributions proceeded in three stages. First, at each energy the logarithm of the incident charge-state population  $\phi_\alpha$  was plotted as a function of the target thickness  $x$ . The best straight line of the form

$$\phi_\alpha(x) = \phi_\alpha(0) e^{-s_\alpha x} \quad (5)$$

was determined by eye, where the slope  $s_\alpha$  is the first-order approximation to the sum of the cross sections  $k_\alpha$ , as given with the restrictions of Eq. (2). An example of these semilogarithmic decay plots is shown in Fig. 2 for all incident charge

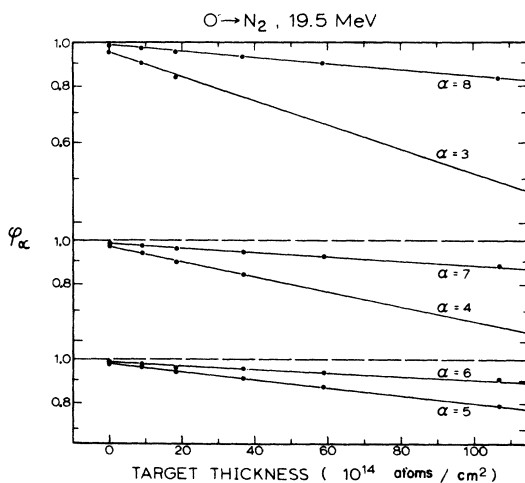


FIG. 2. Incident charge state population  $\phi_\alpha$  as a function of gas target thickness for 19.5-MeV oxygen ions passing through nitrogen gas. The slopes of the straight lines in the figure are the total charge-exchange cross sections  $s_\alpha$  given in Eq. 5.

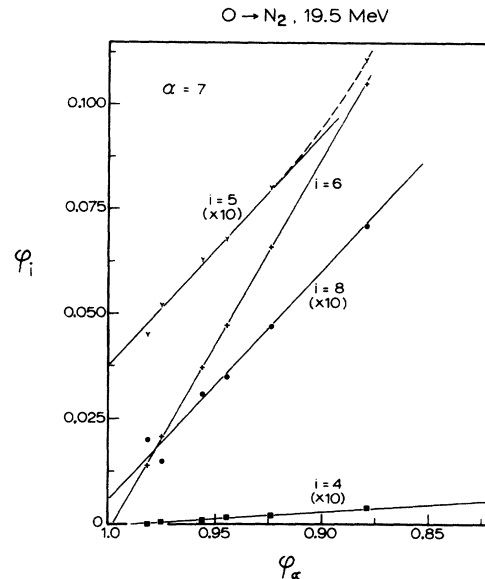


FIG. 3. Growth of various charge states  $\phi_i$  in nitrogen gas as a function of the decay of the incident +7 oxygen ions at 19.5 MeV. The data points at each value of  $\phi_\alpha$  represent a charge distribution measured at one target pressure and the slopes of the lines are equal to the relative charge-exchange cross sections  $\sigma_{\alpha i}/k_\alpha$  given in Eq. (2b).

states from +3 to +8 of 19.5-MeV oxygen ions passing through nitrogen gas. It can be seen that  $\phi_\alpha(0)$  is not unity but ranges from 0.97 to 0.99 as described in Sec. II. In the approximation of Eq. (2) this should have no effect on the "slope"  $s_\alpha$ . It is evident from the figure that a simple exponential decay appears to hold for  $\phi_\alpha$  even as low as 0.8 for some charge states—much farther than one would expect that Eq. (2) would hold. However, this is in agreement with Eq. (4) for those incident charge states for which  $a_\alpha$  is small.

Also, the observed exponential decay in the incident charge state was used to adjust certain data taken at low pressures in argon gas. These data were inaccurate because of the insensitivity of the high-pressure ionization gauge below  $3 \times 10^{-4}$  Torr. At low pressure, the target thickness  $x$  was chosen by fitting  $\phi_\alpha$  for a slowly decaying state (such as  $\phi_8$  or  $\phi_7$ ) to the exponential decay for that state. Since measurements for all charge states were taken without changing gas pressure, the attenuation of the rapidly decaying states (such as  $\phi_3$ ) could be determined relative to that of the slowly decaying ones. The magnitude of the cross sections for the latter was determined using data from the higher-pressure region where the ionization gauge was calibrated.

A second step in the data analysis was the determination of the relative cross sections  $\sigma_{\alpha i}/k_\alpha$  which, according to Eq. (2b), can be determined

from the slope of a plot of  $\phi_i$  as a function of  $(1 - \phi_\alpha)$ . In Fig. 3 such a plot is shown for 19.5-MeV oxygen + 7 ions in nitrogen gas. The extraction of individual cross sections from plots such as this has great advantages over the usual technique of plotting  $\phi_i$  as a function of target thickness.<sup>13</sup> Most important, it should be noted that no gas pressure measurement is used in making graphs such as Fig. 3 and therefore the relative cross sections can be determined to the accuracy of the counting measurements. Very small relative cross sections corresponding to triple and even quadruple electron capture were readily determined from these linear growth plots. These plots also compensate for the curvature introduced into the usual plots of  $\phi_i(x)$  because of the deviation of the quantity  $\phi_\alpha(x)$  from a linear function of  $x$ . Furthermore, when terms other than  $\sigma_{\alpha i} \phi_\alpha$  begin to be important in Eq. (1) (corresponding to more than one collision in the target), curvature will begin to show in such plots. This effect can be seen in Fig. 3 for  $i = 5$  in the region of  $\phi_\alpha \sim 0.9$ . In extracting the relative cross sections from these growth plots, care was taken to consider linear growth asymptotically from  $\phi_\alpha \sim 1.0$ .

The third step in the data analysis was the correction of the slope  $s_\alpha$  to obtain the total cross section  $k_\alpha$  using Eqs. (4a) and (5) to obtain

$$\frac{k_\alpha}{s_\alpha} = \frac{1}{(1 + a_\alpha)} \frac{\ln[(1 + a_\alpha) \phi_\alpha(x)/\phi_\alpha(0)] - a_\alpha}{\ln[\phi_\alpha(x)/\phi_\alpha(0)]}. \quad (6)$$

Under the first-order assumption that  $k_\alpha \approx s_\alpha$  the correction parameter  $a_\alpha$  was computed using Eq. (4b) and the relative cross sections  $\sigma_{\alpha i}/k_\alpha$ . For the dominant charge states at each energy, the values of  $a_\alpha$  range from 1.3 to 1.7, and for the less probable states they are considerably smaller, being approximately zero for charge states two units from the most probable charge. In Fig. 4 is shown a plot of  $k_\alpha/s_\alpha$  as a function of the correction parameter  $a_\alpha$  with  $\phi_\alpha(x)/\phi_\alpha(0) = 0.9$  in Eq. (6). For

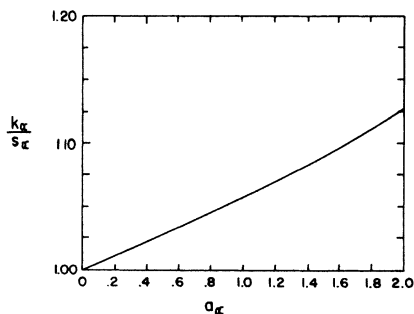


FIG. 4. Ratio of the total charge-exchange cross section  $k_\alpha$  to the first order estimates  $s_\alpha$  plotted as a function of the correction parameter  $a_\alpha$ . The smooth curve represents Eq. (6) with  $\phi_\alpha(x)/\phi_\alpha(0) = 0.9$ .

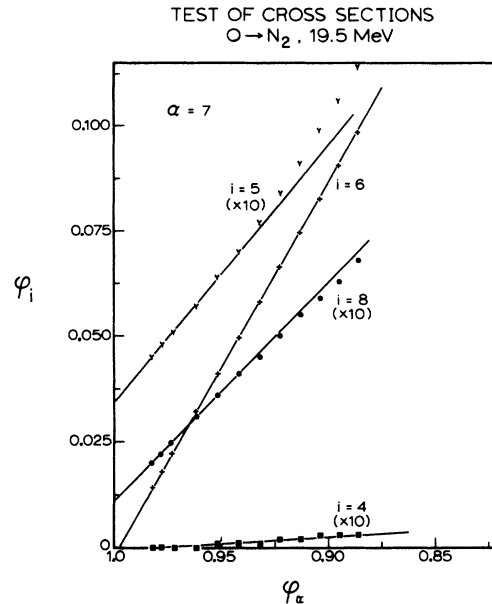


FIG. 5. Charge distributions calculated from the experimental cross sections for 19.5-MeV + 7 oxygen ions in nitrogen gas. The onset of a quadratic growth of  $\phi_5$  is evident for  $\phi_7 < 0.92$ .

oxygen + 6 ions in nitrogen at 16 MeV,  $k_\alpha$  was 11% greater than  $s_\alpha$  and this was the largest correction found. More typically,  $k_\alpha$  was approximately 3% greater than  $s_\alpha$ . Lastly, the complete set of charge-exchange cross sections at each energy was determined from the relative cross sections  $\sigma_{\alpha i}/k_\alpha$  and the total cross sections  $k_\alpha$ .

### C. Reliability

In order to test that this analysis technique did give reliable results, even for the small multiple-transfer cross sections, a computer program was written to generate the charge-state populations as a function of target thickness from the experimentally determined cross sections and initial conditions. A reanalysis of these calculated distributions using the technique described above gave close agreement with the experimental data without the usual random variations. An example of the calculated distributions is shown in Fig. 5 in which the growth curves corresponding to the experimental data in Fig. 3 are shown. Relative cross sections extracted from Fig. 5 are the same as for Fig. 3 even for the small triple-electron capture labeled by  $i = 4$ .

The identification of the multiple-transfer cross sections rather than two-collision processes rests on the linearity of the growth of the appropriate charge state as a function of the decay of the incident state. This linearity near the origin for the very small relative cross sections is impossible

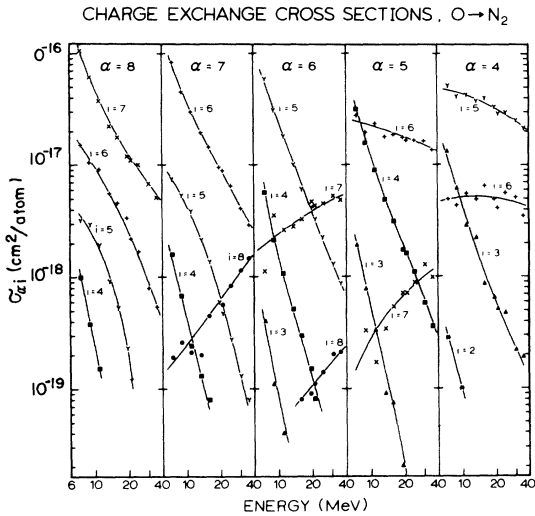


FIG. 6. Set of charge-exchange cross sections  $\sigma_{\alpha i}$  for oxygen ions in argon plotted as a function of energy. The separate sections of the plot are for different initial states  $\alpha$ , and the smooth curves through the data points are labeled by the final states  $i$ .

to judge from Figs. 3 or 5. However, by setting various multiple-transfer cross sections identically zero in the program and computing the charge distributions, this judgment was easily made. For example, if  $\sigma_{74} = 0$  and the population for 19.5-MeV oxygen + 7 ions in nitrogen gas are calculated, then  $\phi_4 < 0.0002$  even for  $\phi_7 \sim 0.9$ . Clearly the points labeled  $i = 4$  in Figs. 3 and 5 result from the triple-electron-capture cross section  $\sigma_{74}$ .

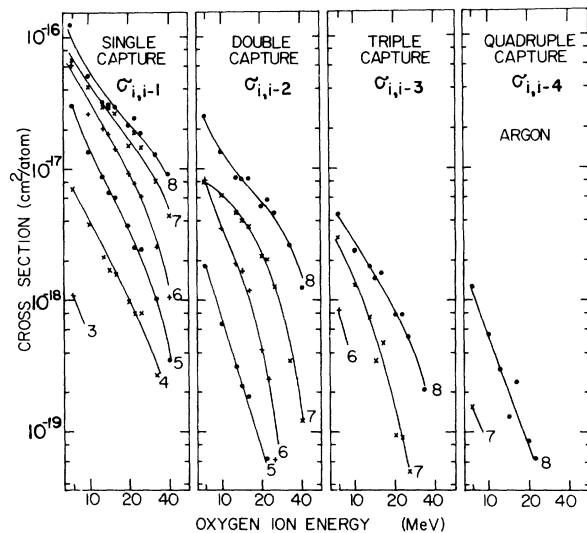


FIG. 7. Electron-capture cross sections for oxygen ions in argon. The smooth curves are labeled by the initial charge state.

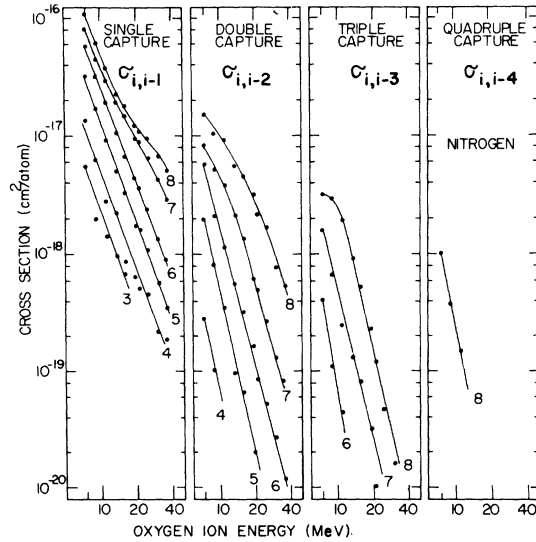


FIG. 8. Electron-capture cross sections for oxygen ions in nitrogen. The smooth curves are labeled by the initial charge state.

These calculations indicate that the analysis technique used in this work introduces negligible error to the total cross sections  $k_{\alpha}$ , which are limited to a precision of 10% by the error in target pressure determination. This method of analysis introduces systematic errors of less than 2% in the relative cross sections  $\sigma_{\alpha i}/k_{\alpha}$ . Experimental random errors associated with the background from slit-edge scattering ranged from a few percent for single transfer to as large as a factor of 2 for transfer of three or four electrons.

#### IV. RESULTS AND DISCUSSION

##### A. General

The complete set of charge-exchange cross sections determined for oxygen ions passing through nitrogen gas is shown in Fig. 6. Measurements were made at ten energies from 7.5 to 36 MeV with incident charge states ranging from the fully stripped +8 to +4 and in some instances (not shown in Fig. 6) to +3 and +2. The separate sections of the figure show the energy dependence of the individual cross sections  $\sigma_{\alpha i}$  for the same initial states  $\alpha$  and are labeled by the final state  $i$ . Smooth curves have been drawn by eye through the experimental points to illustrate the general energy dependence of each  $\sigma_{\alpha i}$ .

A general feature of the cross sections that is evident from Fig. 6 is the existence of multiple-transfer cross sections for all incident charge states. For example, the double-capture cross section  $\sigma_{88}$  is about 15% of the single-capture cross section  $\sigma_{87}$  over a wide energy range, and even the quadruple-capture cross section  $\sigma_{84}$  is about 1% of

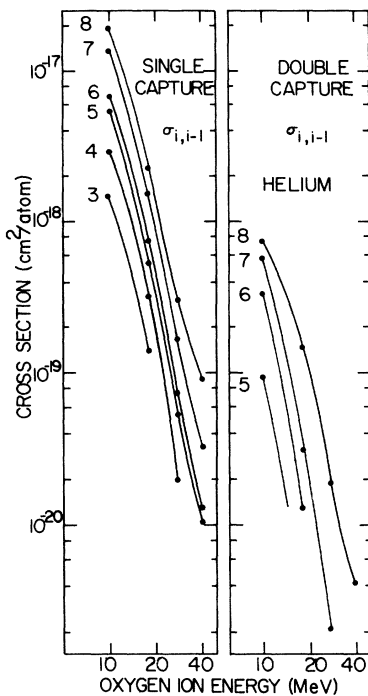


FIG. 9. Electron-capture cross sections for oxygen in helium. The smooth curves are labeled by the initial charge state.

$\sigma_{87}$ . Similarly, the double-loss cross section  $\sigma_{46}$  ranges from 10 to 25% of the single-loss cross section  $\sigma_{45}$ .

In argon gas, charge-exchange cross sections were determined at ten energies from 7.5 to 40 MeV and in helium gas, experiments were performed at four energies from 10 to 40 MeV. The broad features of the cross sections in argon were similar to those in nitrogen, while in helium the cross sections were more than an order of magnitude smaller in general, and the cross sections for more than two electrons transferred in a single collision were not observed.

#### B. Capture Cross Sections

All of the electron-capture cross sections for oxygen ions obtained in this experiment are shown in Fig. 7 for argon, in Fig. 8 for nitrogen, and in Fig. 9 for helium. The charge of the incident ion is the parameter labeled on each curve in the figures. A detailed analysis and interpretation of these data will be published separately<sup>16</sup>; however, a brief discussion of some of the features will be given here.

Perhaps of foremost importance is the large value of the cross sections for capture at high velocity in nitrogen and argon. A comparison of the single-capture cross section for oxygen + 8 ions and protons in argon as functions of velocity is

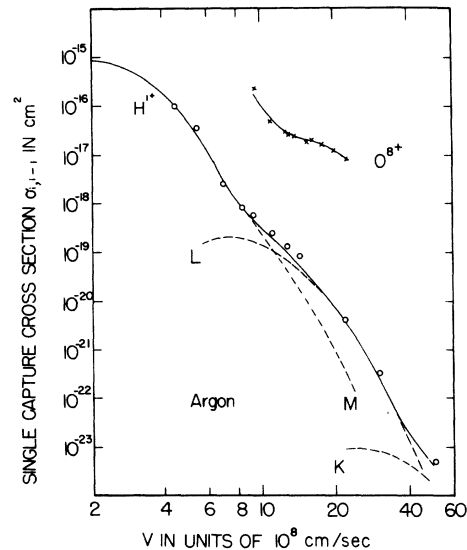


FIG. 10. Electron-capture cross sections for protons and oxygen + 8 ions in argon plotted as a function of velocity. For protons the smooth curve is a theoretical estimate of the cross section (Ref. 17) and the circles are experimental measurements (as summarized in Ref. 4). For oxygen ions the crosses represent the present measurements.

shown in Fig. 10. The solid curve is a theoretical estimate of the capture of electrons by protons including contributions from the inner shells of the argon atom<sup>17</sup>; the open circles are experimental

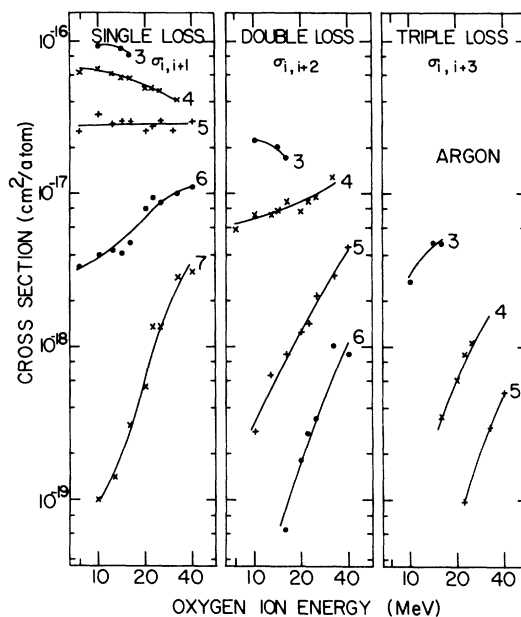


FIG. 11. Electron-loss cross sections for oxygen ions in argon. The smooth curves are labeled by the initial charge state.

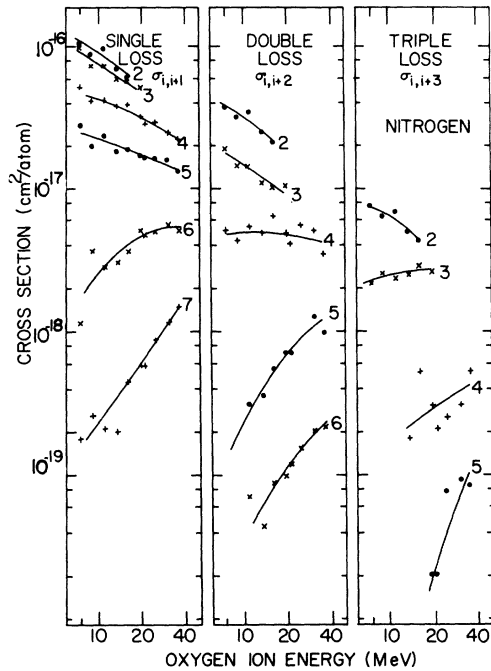


FIG. 12. Electron-loss cross sections for oxygen ions in nitrogen. The smooth curves are labeled by the initial charge state.

cross sections for protons<sup>4</sup>; and the crosses are experimental capture cross sections for bare oxygen nuclei determined in the present work. The capture cross section for oxygen is three orders of magnitude larger than for protons at  $2 \times 10^9$  cm/sec.

Associated with the large value of capture for oxygen is a relatively slow decrease in cross section with energy in the heavy gases. In general, the capture cross sections decrease monotonically, with a dependence ranging approximately from  $V^{-3}$  for  $\sigma_{87}$  in argon to  $V^{-9}$  for  $\sigma_{65}$  in helium. The approximate velocity dependence of the single-capture cross sections for oxygen ions of various charges in the three gases is given in Table I. It is apparent that the velocity dependence is much less in the heavy gases than in helium. The much larger cross sections at high velocity from a collision with an argon or nitrogen atom than with a helium atom suggest that loosely bound electrons are not as

TABLE I. Approximate velocity dependence of single-electron capture cross section from three target gases for oxygen ions faster than  $9 \times 10^8$  cm/sec.

Cross section	Argon	Nitrogen	Helium
$\sigma_{87}, \sigma_{76}$	$V^{-3}, V^{-4}$	$V^{-4}$	$V^{-8}$
$\sigma_{65}, \sigma_{54}, \sigma_{43}$	$V^{-5}$	$V^{-5}, V^{-6}$	$V^{-9}$

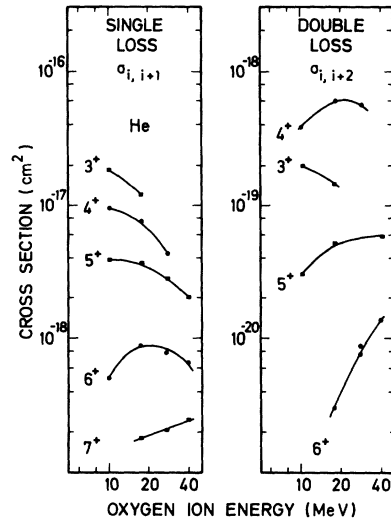


FIG. 13. Electron-loss cross sections for oxygen ions in helium. The smooth curves are labeled by the initial charge state.

likely to be captured as those more tightly bound in the atom initially.

A second feature of the oxygen cross sections shown in Table I is the weaker velocity dependence for the +7 or +8 ions than for lower charge states. The correlation of the larger capture cross sections with the +7 and +8 ions suggests that capture into vacant levels in the *K* shell of the oxygen ion is a more probable event than capture into the levels of the outer shell at high velocities.

Another interesting characteristic of the cross sections shown in Figs. 7, 8, and 9 is the existence of large multiple-capture cross sections in nitrogen and argon. These necessarily indicate an appreciable probability of electron capture in a given single collision. The large single-capture cross sections observed in these gases therefore do not result from the integration of low-probability interactions over a large region of impact parameter, but rather must be associated with interactions of short range, possibly between inner shells.

### C. Electron-Loss Cross Sections

The electron-loss cross sections for oxygen ions obtained in this experiment are shown in Fig. 11 for argon, in Fig. 12 for nitrogen, and in Fig. 13 for helium. Each curve is labeled with the charge of the incident ion. In general, from the work of Bohr<sup>18</sup> and Bohr and Lindhard<sup>19</sup> the loss cross sections are better understood than the capture cross sections, and are expected to have a maximum when the ion velocity  $V$  and the velocity  $u$  of the electron about to be lost are related by  $V = \gamma u$ , where  $\gamma$  is slightly larger than unity.

For oxygen *K*-shell electrons to be lost from the

+6 or +7 ion,  $V/u \sim 1$  at  $E \sim 25$  MeV. For the +6 oxygen ions in helium gas,  $\sigma_{67}$  does go through a broad maximum in this region, while in nitrogen the maximum appears to have been reached at about 30 to 40 MeV, and in argon the maximum is being approached by 40 MeV. These observations agree with the previously observed increase in  $\gamma$  with the atomic number of the atom.<sup>2</sup> For the +7 ions the loss cross section is rising sharply at 40 MeV in all three target gases and the maximum is out of the range of these experiments.

For the single-electron-loss cross sections of the +5, +4, and lower charged ions,  $V/u \sim 1$  at  $E \sim 4$  MeV. In all three target gases the loss cross section for charge states +4 and lower are slowly decreasing with energy above 7 MeV. The loss cross section of the +5 state in argon is constant from 7 to 40 MeV, while in nitrogen and helium the data are consistent with a maximum in  $\sigma_{56}$  in the region 5–10 MeV.

The multiple-loss cross sections are also rather easily understood if the loss of each electron in the collision occurs as a relatively independent event. Then all the loss cross sections leading to the same final charge state will be similar and relatively independent of the number of electrons lost in the single collision. In the data shown in Figs. 11 and 12 for collisions in argon and nitrogen, the energy dependence of the single- and multiple-loss cross sections leading to the same final state are generally the same, while the magnitude is down by a factor of 2 or 3 for each additional electron lost. However, the double-loss cross sections in helium are reduced by more than an order of magnitude from the corresponding single-loss cross section to the same charge state, and the energy dependence is not so closely related.

It should be pointed out that the experimental error in determining loss cross sections is considerably larger than for capture cross sections because all slit-edge scattering of the beam in passing through the collimators will decrease the energy and such particles will be deflected towards higher ap-

parent charge states in the magnetic spectrometer. The background found for charge states higher than the incident state is always greater than for the lower states. Consequently, the small multiple-loss cross sections are uncertain by as much as a factor of 2.

#### D. Conclusion

Detailed electron-capture and -loss cross sections have been obtained for oxygen ions in argon, nitrogen, and helium gases in the energy interval from 7.5 to 40 MeV. Multiple transfers of as many as four electrons in a single collision have been observed. The analysis used allowed these small multiple cross sections to be extracted reliably from charge distributions determined experimentally using thin-target conditions. The data have been presented with the electron-capture cross sections separate from the loss cross sections in each gas. The loss cross sections are consistent with a model predicting a maximum in the cross section for loss of any electron at an ion velocity comparable to or slightly greater than the orbital velocity of the lost electron. The capture cross sections are not so easily interpreted and further analysis of these data is in progress. However, it is apparent that the binding energies both in the initial and final state of the captured electron play an important role in both the magnitude and energy dependence of the capture cross sections.

#### ACKNOWLEDGMENTS

The authors would like to thank Professor Bent Elbek and the staff at the Tandem Accelerator Lab of the Niels Bohr Institute at Risø for their toleration, cooperation, and support in carrying out these experiments. The support of Professor K. O. Nielsen of Aarhus is gratefully acknowledged. One of us (J. R. M.) acknowledges the financial support of a National Research Council of Canada Fellowship during a post-doctoral appointment when these experiments were performed.

\*Present address: Department of Physics, Kansas State University, Manhattan, Kans. 66502.

†Present address: Department of Physics and Astronomy, University of Maryland, College Park, Md. 20742.

<sup>1</sup>S. K. Allison and M. Garcia Munoz, in *Atomic and Molecular Processes*, edited by D. R. Bates (Academic, New York, 1962), p. 721.

<sup>2</sup>V. S. Nikolaev, *Usp. Fiz. Nauk* **85**, 679 (1965) [Sov. Phys. Usp. **8**, 269 (1965)].

<sup>3</sup>L. C. Northcliffe, *Ann. Rev. Nucl. Sci.* **13**, 67 (1963).

<sup>4</sup>L. M. Welch, K. H. Berkner, S. N. Kaplan, and R. V. Pyle, *Phys. Rev.* **158**, 85 (1967).

<sup>5</sup>L. H. Toboren, R. A. Langley, and M. Y. Nakai, *Phys. Rev.* **171**, 114 (1968).

<sup>6</sup>C. D. Moak, H. O. Lutz, L. Bridwell, L. C. North-

cliffe, and S. Datz, *Phys. Rev.* **176**, 427 (1968).

<sup>7</sup>E. Acerbi, M. Castiglioni, G. Dotto, F. Resmini, C. Succi, and G. Tagliaferri, *Nuovo Cimento* **50B**, 176 (1967).

<sup>8</sup>F. W. Martin, *Phys. Rev.* **140**, A75 (1965).

<sup>9</sup>A preliminary report of the present work was given in *Bull. Am. Phys. Soc.* **13**, 51 (1968).

<sup>10</sup>G. J. Schultz and A. V. Phelps, *Rev. Sci. Instr.* **28**, 1051 (1957).

<sup>11</sup>Ch. Meinke and G. Reich, *Vacuum* **13**, 579 (1963).

<sup>12</sup>E. Laegsgaard, F. W. Martin, and W. M. Gibson, *IEEE Trans. Nucl. Sci.* **NS-15-3**, 239 (1968).

<sup>13</sup>G. Ryding, A. B. Wittkower, and P. H. Rose, *Phys. Rev.* **185**, 129 (1969).

<sup>14</sup>I. A. Sellin, B. L. Donnally, and C. Y. Fan, *Phys.*

Rev. Letters 21, 717 (1968).

<sup>15</sup>I. S. Dmitriev, V. S. Nikolaev, and Ya. A. Teplova, Phys. Letters 26A, 122 (1968).

<sup>16</sup>F. W. Martin and J. R. Macdonald, following paper, Phys. Rev. A 4, 1974, (1971).

<sup>17</sup>V. S. Nikolaev, Zh. Eksperim. i Teor. Fiz. 51, 1263

(1966) [Sov. Phys. JETP 24, 847 (1967)].

<sup>18</sup>N. Bohr, Kgl. Danske Videnskab. Selskab Mat. Fys. Medd. 18, No. 8 (1948).

<sup>19</sup>N. Bohr and J. Lindhard, Kgl. Danske Videnskab. Selskab Mat. Fys. Medd. 28, No. 7 (1954).

PHYSICAL REVIEW A

VOLUME 4, NUMBER 5

NOVEMBER 1971

## Electron-Capture Processes of 10–40-MeV Oxygen Ions in Helium, Nitrogen, and Argon

F. W. Martin\*

*Institute of Physics, University of Aarhus, Aarhus, Denmark*

and

J. R. Macdonald†

*Niels Bohr Institute, Copenhagen, Denmark*

(Received 3 May 1971)

Experimental data on electron-capture cross sections are analyzed in order to obtain the cross sections for removal of  $n$  given atomic electrons, where  $n=1, 2$ , or  $3$ . Probabilities of capture averaged over certain regions of impact parameter are obtained from ratios of these cross sections. Maxima are found in the capture probabilities for  $+8$  oxygen ions in helium, and for  $+8$  and  $+7$  ions in nitrogen and argon. No maxima are found for ions of lower charge. The large cross sections at high velocities in nitrogen and argon are attributed to capture from the  $K$  shell of nitrogen and the  $L$  shell of argon, which contain electrons with momenta great enough to satisfy conservation requirements. The larger cross sections for  $+8$  ions and the maxima in capture probability are attributed to exoergic capture from atomic energy levels into the deeply bound  $K$  shell of the oxygen  $+8$  ion. A criterion based on an atomic-orbital theory is given for the velocity at which maxima due to exoergic capture should occur, and this is in rough agreement with the observed velocities. Electron-capture cross sections from atoms with tightly bound shells can generally be expected to be large for heavy ions even at velocities greater than  $10^9$  cm/sec.

### I. INTRODUCTION

Electron capture in atomic collisions has been extensively studied for ions with 1–100 keV of energy per nucleon. Typically the cross section has a maximum as great as  $10^{-15}$  cm<sup>2</sup> at 1–40 keV per nucleon and falls as the inverse fourth to seventh power of the ion velocity.<sup>1–5</sup> At higher velocities, capture has been studied for protons and exhibits an inverse twelfth-power dependence in hydrogen.<sup>6</sup> An inverse eighth-power dependence on velocity was observed for protons in argon, in which the inner shells contain electrons with velocities greater than that of the projectile.<sup>6</sup>

In a previous paper, the authors have presented experimental measurements of electron-capture and electron-loss cross sections for high-energy oxygen ions.<sup>7</sup> A major difference of the capture process in this case from that for high-energy protons is the increased binding energy of the captured electron. It is possible that the binding energy in the ion may be greater than that in the target atom, resulting in an exoergic type of

transfer. In addition, for certain atomic shells and ionic binding energies, the difference in binding energies may equal  $\frac{1}{2}mV^2$ , where  $m$  is the mass of the electron and  $V$  is the velocity of the ion, and for reasons discussed below a large capture cross section is anticipated at this velocity. The previous experimental measurements were conducted at energies for which this criterion is satisfied, for electron transfer both from atoms which contain electrons with the velocity of the projectile and from those which do not.

In the following analysis a method of calculating the probability of capture of a given electron from cross sections involving capture from a whole atomic shell is presented, and values of these probabilities are computed from experimental data. The effects of conservation of momentum of the captured electron are discussed, and the possibility of a maximum in the probability of capture for exoergic transitions is pointed out on theoretical grounds. Finally the data are discussed with regard to various transitions among the shells of the collision partners.